

## Potent antiplasmodial alkaloids from the rhizobacterium *Pantoea agglomerans* as hemozoin modulators

Bathini Thissera,<sup>1</sup> Irene Hallyburton,<sup>2</sup> Che Julius Ngwa,<sup>3</sup> Hafsa Cherif-Silini,<sup>4</sup> Ahmed S. I. Hassane,<sup>5</sup> Mark Anderson,<sup>2</sup> Lorna A Campbell,<sup>2</sup> Nicole Mutter,<sup>2</sup> Manal Eshelli,<sup>1,6</sup> Usama R. Abdelmohsen,<sup>7,8</sup> Mohammed Yaseen,<sup>1</sup> Gabriele Pradel,<sup>3</sup> Lassaad Belbahri,<sup>9</sup> Bahaa Elgendy,<sup>10,11</sup> Lamees Hegazy,<sup>10,\*</sup> Mostafa E. Rateb<sup>1,\*</sup>

<sup>1</sup> School of Computing, Engineering and Physical Sciences, University of the West of Scotland, PA12BE Paisley, UK

<sup>2</sup> Drug Discovery Unit, Wellcome Centre for Anti-infective Research, University of Dundee, Dow Street, Dundee DD1 5EH

<sup>3</sup> Division of Cellular and Applied Infection Biology, Institute of Zoology, RWTH Aachen University, 52074 Aachen, Germany.

<sup>4</sup> Laboratory of Applied Microbiology, Department of Microbiology, Faculty of Natural and Life Sciences, Ferhat Abbas University, Setif 19000, Algeria

<sup>5</sup> Aberdeen Royal Infirmary, Foresterhill health campus, Foresterhill Road, Aberdeen AB25 2ZN, Scotland, UK

<sup>6</sup> Food Science and Technology Department, Faculty of Agriculture, University of Tripoli, Tripoli 13275, Libya

<sup>7</sup> Department of Pharmacognosy, Faculty of Pharmacy, Minia University, Minia 61519, Egypt

<sup>8</sup> Department of Pharmacognosy, Faculty of Pharmacy, Deraya University, Minia 61519, Egypt

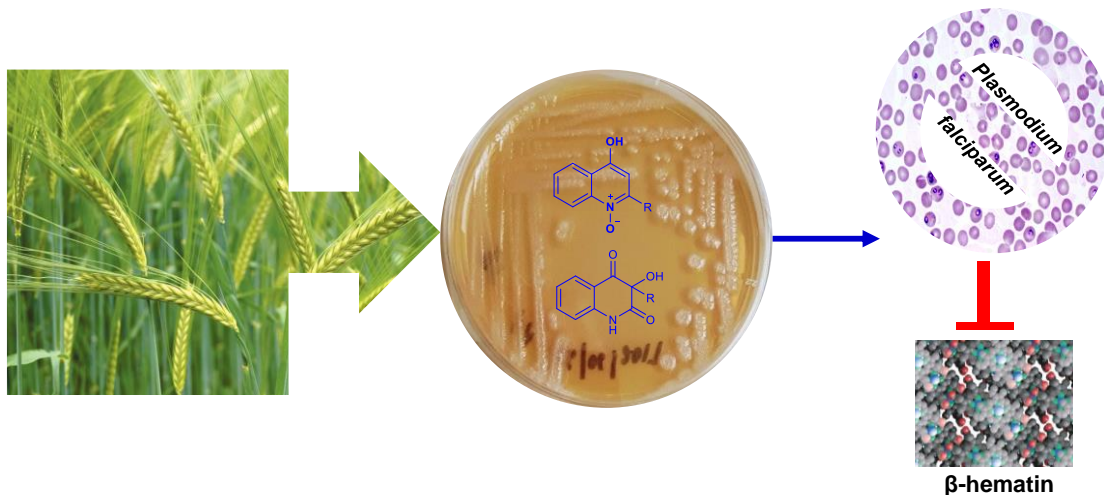
<sup>9</sup> Laboratory of Soil Biology, University of Neuchatel, 2000 Neuchatel, Switzerland

<sup>10</sup> Center for Clinical Pharmacology, Washington University School of Medicine and University of Health Sciences and Pharmacy, St. Louis, MO 63110, USA

<sup>11</sup> Chemistry Department, Faculty of Science, Benha University, Benha 13518, Egypt

\* **correspondence** to Dr Mostafa E. Rateb (Tel +441418483072; email [Mostafa.Rateb@uws.ac.uk](mailto:Mostafa.Rateb@uws.ac.uk)) and Dr Lamees Hegazy (Tel +13144468475; email: [lamees.hegazy@uhsp.edu](mailto:lamees.hegazy@uhsp.edu)).

### GRAPHICAL ABSTRACT



## ABSTRACT

Global health concern regarding malaria has increased since the first report of artemisinin-resistant *Plasmodium falciparum* (Pf) two decades ago. The current therapies suffer various drawbacks such as low efficacy and significant side effects, alarming for an urgent need of more effective and less toxic drugs with higher patient compliance. Chemical entities with natural origins become progressively attractive as new drug leads due to their structural diversity and bio-compatibility. This study initially aimed at the targeted isolation of hydroxyquinoline derivatives following our published genomics and metabolomics study of *Pantoea agglomerans* (Pa). Fermentation of Pa on a pre-selected medium followed by chromatographic isolation, NMR and HRMS analyses led to the characterisation of one new hydroxyquinoline alkaloid together with another six known congeners and two known hydroxyquinolone derivatives. When screened for their antimalarial activity by high throughput screening against asexual blood-stage parasites, almost all compounds showed potent and selective sub-micromolar activities. Computational investigation was performed to identify the antiplasmodial potential targets. Ligand-based similarity search predicted the tested compounds to act as hemozoin inhibitors. Computational target identification results were further validated by competitive hemozoin inhibitory properties of hydroxyquinoline and hydroxyquinolone derivatives *in vitro*. The overall results suggest this natural scaffold is of potential to be developed as antimalarial drug lead.

**Key words:** *P. agglomerans*, hydroxyquinoline, hydroxyquinolone, *Plasmodium*, hemozoin.

### 1. Introduction

In the 21<sup>st</sup> century, malaria has re-emerged as a serious global health condition and has drawn WHO attention to introduce “Rollback malaria programme” to set up crucial measures. The measures included widening the use of antimalarial drug Artemisinin. This drug is the most effective commercially available therapy first isolated from the Chinese plant *Artemisia annua* [1]. According to the malaria report published by WHO in 2019 (<https://www.who.int/publications/i/item/world-malaria-report-2019>), an estimated 228 million cases were reported worldwide in 2018 of which 93% cases belong to the African Region and 405,000 fatalities globally. In the same report, WHO statistics highlight that

*Plasmodium falciparum* (Pf) is the most predominant malaria parasite in African, South- East Asia and Eastern Mediterranean regions. The global concern regarding Pf developing resistance to artemisinin agents has been evolving swiftly since the first report in South East Asia [2, 3, 4]. On the other side, the malaria parasites, *Plasmodium* spp. have developed resistance to many other current therapies (Figure 1) such as chloroquine and sulfadoxine/pyrimethamine leading to a crisis in many African nations and other malaria-endemic countries [5]. Artemisinin-based combination therapies are the recommended first-line treatments of malaria. Unfortunately, concerns have been raised that such treatments' efficacy has declined, threatening to compromise global endeavours to eradicate this disease [6,1]. Thus, there is an urgent need for effective and safe new antimalarial therapies.

Microorganisms possess an outstanding ability to produce bioactive secondary metabolites (SMs). They have already contributed some of the most important products into the pharmaceutical industry such as statins, antibacterial, anti-parasitic, anticancer and anthelmintic treatments [7, 8]. The ability of microbial SMs to target specific cellular sites is mainly featured by its naturally optimised structures to perform specific biological functions [9]. The application of genome mining facilitates the identification of effective bacterial strains for targeted isolation of SMs with the aid of metabolomics tools [10]. *Pantoea agglomerans* (Pa) is a Gram-negative epiphyte of a wide range of plants and belongs to the family *Enterobacteriaceae* [11]. The strain Pa is a well-known biocontrol for fire blight caused by *Erwinia amylovora* from the same family *Enterobacteriaceae* [11]). Following an investigation based on genomics and metabolomics [10], the rhizobacterium strain Pa was identified as a talented strain to produce diverse SMs with therapeutic significances. These findings encouraged us to perform targeted isolation of quinoline derivatives to discover new metabolites that could replace or resemble the currently used quinoline-derived antimalarial therapies (Figure 1). According to WHO, quinine, quinidine, chloroquine, mefloquine, primaquine, amodiaquine are widely used for malaria treatment (<https://www.who.int/groups/expert-committee-on-selection-and-use-of-essential-medicines/essential-medicines-lists>) but most of them are acquiring resistance against Pf [12]. This work presents isolation and structural characterisation of one new and six known hydroxyquinoline derivatives and two known hydroxyquinolones and their selective growth inhibitory effect against Pf as the main causative agents

of malaria. Also, investigation of potential targets using ligand-based similarity search and *in vitro* target validation were executed leading to further investigations.

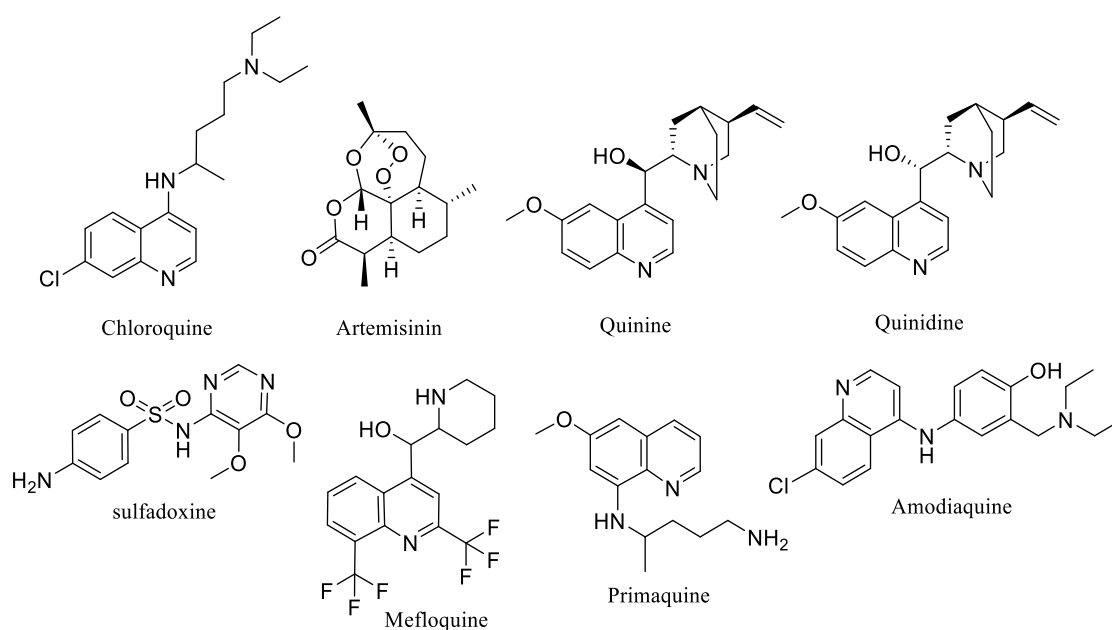


**Figure 1.** Current therapies for malaria.

## 2. Materials and methods

### 2.1. Strain isolation

The strain was isolated as an endophyte of Durum wheat root by collecting the rhizosphere with intact wheat roots in the arid Bou-Saâda region, south Algeria (35°23'38"N4°19'18.1"E) [10, 14].

### 2.2. Fermentation and Isolation

Strain Pa bacterial glycerol stock was cultured in agar plates with ISP2 medium and incubated 48 hours at 25 °C. The medium optimisation was performed under OSMAC (One Strain Many Compounds) condition followed by metabolomics-assisted PCA analysis [10] (Figure SI 7). The modified ISP2 medium (M1), reported as the best medium to produce that array of alkyl hydroxyquinoline analogues with possible new hits [10], was used for large scale production of these metabolites in the current study.

For large scale production, 10L of ISP2 modified medium (M1) (malt extract 4 g/L, yeast extract 4 g/L, glucose 4 g/L, lab Lemco 2 g/L) was prepared and splitted into 40 × 1L Erlenmeyer flasks containing

300mL each, autoclaved and inoculated under aseptic conditions. The production flasks were fermented for eight days at 25 °C on a rotary shaker at 180 rpm. Then approximately 50g/L HP20 resins (Sigma-Aldrich Company Ltd, Supelco UK) was added to each flask and left shaking for another 6 hours before harvesting. The whole culture was then harvested, followed by centrifugation at 10,000 rpm for 5 min. The residue containing the HP20 beads and bacterial cell mass was washed further with water to remove the medium completely. This residue was soaked in MeOH for 24 hours and then with acetone for another 24 hours. Both solvents were combined and evaporated under vacuum to produce 12.8g of dark brown semi-solid. Total extract of Pa was then dissolved in 50:50 MeOH/H<sub>2</sub>O and fractionated with hexane, CH<sub>2</sub>Cl<sub>2</sub> and EtOAc (Fisher Scientific UK Ltd, Leicestershire, UK) successively to produce three fractions. Each fraction was screened on TLC deemed CH<sub>2</sub>Cl<sub>2</sub> and EtOAc were similar and hence combined. The combined fractions was then subjected to semi-preparative HPLC purification (sunfire™, prep C18, 5µm, 10 × 250mm), eluted with a gradient system of 10% - 100% CH<sub>3</sub>CN (Rathburn Chemicals Ltd, Scotland, UK) in H<sub>2</sub>O over 75min and 5min at 100% CH<sub>3</sub>CN at a flow rate of 1.5mL/min to yield a series of hydroxyquinolines **1** (tr 54.5min, 4mg), **2** (tr 53.3min, 6mg), **3** (tr 45.3min, 3.5mg), **4** (tr 47.9min, 7mg), **5** (tr 52.5min, 3.6mg), **6** (tr 55.3min, 3.6mg), **7** (tr 52.5 min, 6.5mg), **8** (tr 48.5min, 4mg) and **9** (tr 50.0min, 8mg) for the first time from *P. agglomerans* strain Pa.

**Compound 6:** Dark brown semi-solid; UV (MeOH)  $\lambda_{\max}$  (log  $\epsilon$ ): 217 (3.90), 236 (4.20), 316 (3.50), 326 (3.70);  $\delta_{\text{H}}$ /ppm (600 MHz, DMSO-*d*<sub>6</sub>), 5.97 (1H, s), 8.05 (1H, d (*J*=8.1), Ar-H), 7.30 (1H, t (*J*=7.5), Ar-H), 7.65 (1H, t (*J*=7.6), Ar-H), 7.54 (1H, d (*J*=8.4), Ar-H), 6.38 (1H, d (*J*=11.5), 6.09 (1H, m), 2.35-1.44 (2H, m), 1.23-1.30 (10H, m), 0.81 (3H, t (*J*=5.2),  $\delta_{\text{C}}$ /ppm (150 MHz, DMSO-*d*<sub>6</sub>), 13.6, 22.5, 28.7, 28.8, 29.2, 31.7, 33.1, 108.5, 118.8, 123.3, 123.4, 124.8, 125.0, 132.4, 140.3, 140.6, 147.2, 177.1, HRESIMS [M+H]<sup>+</sup> at *m/z* 286.1823 (Calc. 286.1802, C<sub>18</sub>H<sub>23</sub>NO<sub>2</sub>)

### 2.3. Antimalarial Screening

Cultures of the widely-used malaria reference strain of chloroquine-sensitive *Plasmodium falciparum* strain 3D7 were maintained in a 5% suspension of A+ human red blood cells (obtained from East of Scotland Blood Transfusion Service, Ninewells Hospital, Dundee). The strain was cultured in RPMI 1640 medium (pH 7.3) supplemented with 0.5% Albumax II (Gibco Life Technologies, San Diego,

CA), 12 mM sodium bicarbonate, 0.2 mM hypoxanthine, and 20 mg/L gentamicin at 37°C, in a humidified atmosphere of 1% O<sub>2</sub>, 3% CO<sub>2</sub> with a balance of nitrogen. Growth inhibition was quantified using a fluorescence assay utilising the binding of SYBR Green I to double-stranded DNA, which emits a fluorescent signal at 528nm after excitation at 485nm. The assay was performed in 384-well format using a modification of that previously published, namely the use of 1.25% Haematocrit [15, 16].

#### **2.4. Mammalian Toxicity Screening**

A counter-screen was carried out to exclude non-selective and toxic compounds. This was performed using Hep G2 (Human Caucasian hepatocyte carcinoma, HPACC cat.no. 85011430) as indicators for general mammalian cell toxicity. Cells were plated and incubated overnight to allow them to adhere as monolayers. A working stock of each test compound was transferred to an intermediate 384-well plate and pre-diluted with minimum essential media (MEM). The pre-diluted stocks were then transferred onto the cell monolayers, and the plates were incubated for 68 h. Resazurin, to a final concentration of 50µM was added to each well, after which plates were incubated for a further 3 h and measured for fluorescence ( $\lambda_{ex}=528$  nm,  $\lambda_{em}=590$  nm). A standard reference compound, doxorubicin, was included on counterscreen plates to monitor the quality of the assay (potency range 200-400nM). Plates for parasite and mammalian screening assays were prepared in the University of Dundee, Drug Discovery Unit using a Labcyte Echo, Acoustic dispenser. (<https://www.labcyte.com/>)

#### **2.5. In vitro Cell Assay Data Analysis. (Pf and Hep G2)**

All data were processed using IDBS ActivityBase (<https://www.idbs.com/discover-e-workbook/activitybase/>). Raw data were converted into per cent inhibition through linear regression by setting the high inhibition control as 100% and the no inhibition control as 0%. EC<sub>50</sub> curve fitting employed a four-parameter logistic dose-response curve (model 205):

$$y=A + \frac{B-A}{1+(C/x)^D}$$

Where A= % inhibition at bottom, B=% inhibition at top, C- EC<sub>50</sub>, D= Slope, x= inhibitor concentration and y=% inhibition. If curve definition was poor B was fixed to 100.

## 2.6. *In vitro* $\beta$ -Hematin Formation Assay

The principle for  $\beta$ -Hematin formation assay was done by incubating the drug with hemin chloride and triggering its effect on hemozoin polymerisation. Briefly, hemin chloride (100  $\mu$ L of 8 mM in DMSO), 100  $\mu$ L of different concentrations of each test compound (0.8–40 mM) was added in the Eppendorf tube. Control tubes were allocated and treated with D/W instead of the test compound.  $\beta$ -Hematin formation was then started by adding acetate buffer (200  $\mu$ L of 8 M, pH = 5). Later, the tubes were incubated at 37°C for 18 hours, centrifuged (3000 g), and the pellet was collected. The pellet was then dissolved in DMSO and recentrifuged again to get rid of the unreacted hematin, which suspends in the supernatant, giving the second pellet which contains the pure  $\beta$ -hematin. NaOH (400  $\mu$ L of 0.1 N) was added to each tube to dissolve  $\beta$ -hematin, and 100  $\mu$ L aliquots of the final solution were transferred to other tubes, diluted 4 times using NaOH in the same mentioned concentration, and the absorbance was measured using a visible-light spectrophotometer at 390 nm. Chloroquine in the same concentration range was used as a positive control and absorbance versus concentration curve of each test compound compared with chloroquine [*In Vitro* Anti-plasmodium and Chloroquine Resistance Reversal Effects of Andrographolide, Evidence-Based Complementary and Alternative Medicine].

The results were recorded as % inhibition (I%) of heme polymerisation/crystallisation compared to a positive control (chloroquine) using the following formula:  $I\% = [(AB- AA)/AB] 100$ , where AB: absorbance of negative control; AA: absorbance of test compound. The  $IC_{50}$  value of each compound was calculated by using GraphPad Prism 6.0 software.

## 3.0. Results and discussion

### 3.1. Chemical analysis of SMs produced by strain Pa

One Strain Many Compounds (OSMAC) approach was applied to unveil the full metabolic capacity of the Pa strain using six different media (M1-M6). LC-HRESIMS metabolomics analysis of these six media was performed using MZmine 2.37 followed by PCA analysis through SIMCA 14.1 demonstrated diverse chemical profiles. Based on PCA analysis, distribution of score plots and loading plots (Figure

SI-7) highlighted a fairly distinct profile for M1. Dereplication of LC-HRESIMS profile of M1 predicted a new quinoline derivative as well as other known and new hits [10]. Large scale fermentation on M1 medium, extraction with MeOH, liquid-liquid fractionation followed by HPLC purification of the CH<sub>2</sub>Cl<sub>2</sub> fraction led to the isolation of nine hydroxyquinoline analogues (Figure 2), including seven 4-hydroxyquinoline derivatives; 2-*n*-heptyl-4-hydroxyquinoline (**1**) [21], 2-*n*-nonyl-4-hydroxyquinoline (**2**) [13], 2-(*E*)-Non-1'-enyl-4-hydroxyquinoline (**3**) [13], 2-*n*-heptyl-4-hydroxyquinoline-*N*-oxide (**4**) [21], 2-*n*-nonyl-4-hydroxyquinoline-*N*-oxide (**5**) [13], 2-[(*Z*)-undec-4'-enyl]-4-hydroxyquinoline-*N*-oxide (**7**) [13] with one new 2-(*E*)-Non-1'-enyl-4-hydroxyquinoline-*N*-oxide (**6**) in addition to two known 3-hydroxyquinoline derivatives; 3-*n*-heptyl-3-hydroxy-1,2,3,4-tetrahydroquinoline-2,4-dione (**8**) [17] and 2-heptyl-3-hydroxy-4(1*H*)-quinoline (**9**) [18]. All the isolated compounds were fully characterized by 1D, 2D NMR and LC-HRESIMS spectral data analysis and according to literature data.

The new compound **6** was obtained as a dark brown semi-solid, and HRESIMS analysis revealed its quasi-molecular ion peak at *m/z* 286.1823, assigned C<sub>18</sub>H<sub>23</sub>NO<sub>2</sub> as its molecular formula. The <sup>1</sup>H and <sup>13</sup>C NMR (Figure SI 1 and 2) data of the new compound **6** was almost similar to compound **5** except resonances corresponding to two additional low field olefinic protons [ $\delta_{\text{H}}$  6.38 (1H, m, H-1'), [ $\delta_{\text{H}}$  6.09 (1H, m, H-2')] and their respective carbons C-1' ( $\delta_{\text{C}}$  123.4) and C-2' ( $\delta_{\text{C}}$  136.9) (SI Table 1). Similar to all the other eight compounds, an ortho-disubstituted benzene ring was assigned based on the coupling constants of four aromatic resonances [ $\delta_{\text{H}}$  8.05 (1H, d, *J*= 8.1, H-5)], [ $\delta_{\text{H}}$  7.30 (1H, t, *J*=7.5, H-6)], [ $\delta_{\text{H}}$  7.65 (1H, t, *J*= 7.6, H-7)] and [ $\delta_{\text{H}}$  7.54 (1H, d, *J*=8.4, H-8)], in addition to the COSY correlations of H-5 through H-8 (Figure 3). The HMBC correlations from the low field olefinic proton H-3 [ $\delta_{\text{H}}$  5.97 (1H, s)] to C-4a ( $\delta_{\text{C}}$  124.8) and C-5 ( $\delta_{\text{C}}$  125.0) and from H-5 to C-4 ( $\delta_{\text{C}}$  177.1) (Figure 3) confirmed a second ring fused to the benzene ring which was identified as heterocyclic six membered ring with an oxygenated N atom and low field olefinic proton [ $\delta_{\text{H}}$  5.95 (1H, s)] comparable with 4-hydroxyquinoline *N*-oxide moiety. This nucleus was further confirmed by comparison of the <sup>13</sup>C and <sup>1</sup>H NMR data of **6** with the previously reported compounds **4** [21], **5** and **7** [13]. Further analysis of the HMBC correlations from H-2' to C-2 and the COSY correlations H-1' to H-2' (Figure 3) allowed positioning of the alkene



at C-1' as in compound **3**. The length of the alkyl chain was determined by integrating the  $^1\text{H-NMR}$  spectrum and confirmed by mass spectral analysis. The two mass units difference between compound **6** and **5** further verified the presence of a double bond. Upon searching the chemical databases, it was confirmed that this was the first report of compound **6**. The structure was assigned as 2-(*E*)-non-1'-enyl-4-hydroxyquinoline-*N*-oxide.

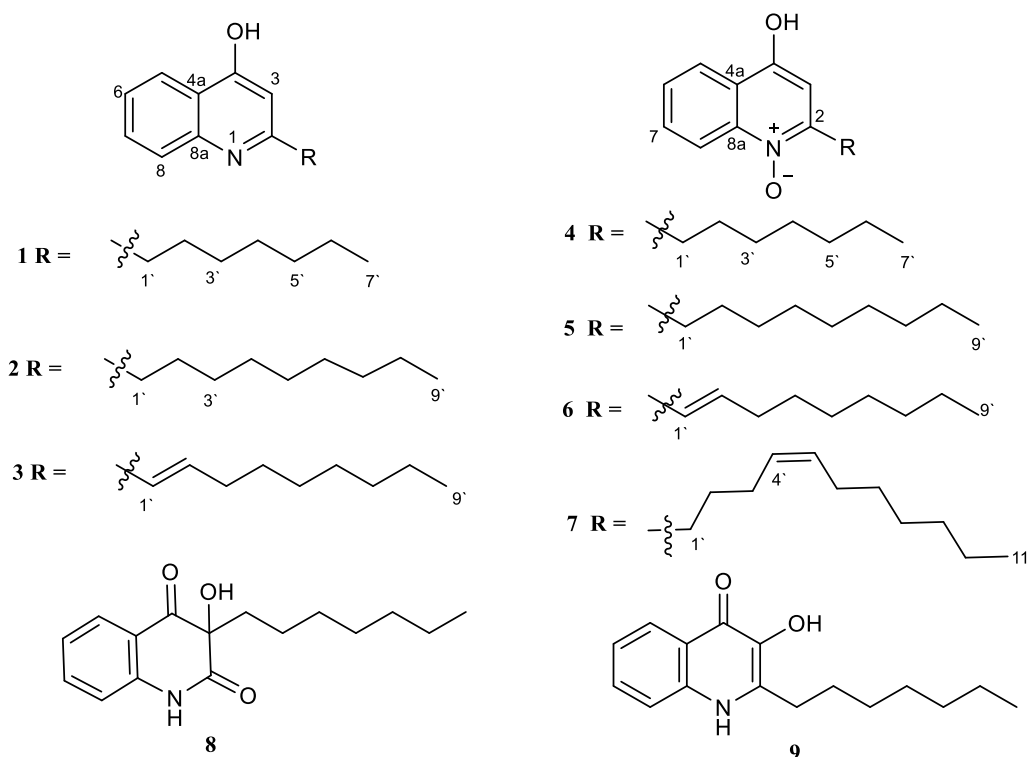


**Figure 2.** Hydroxyquinoline (**1-7**) and hydroxyquinolone (**8-9**) derivatives isolated from Pa.

### 3.2. Antimalarial evaluation of isolated compounds (1-9) against *P. falciparum*

The nine isolated compounds were screened *in vitro* for activity against the asexual blood-stage parasite, and HepG2 cells (human liver carcinoma cells) to determine toxicity against mammalian cells. Almost all compounds demonstrated sub-micromolar activity when tested in the parasite assay containing either 1.25% or 5% erythrocytes by volume (Figure 3). None of the nine compounds tested showed toxicity in the HepG2 assay (Table 1). Three standard drugs, Mefloquine, Pyrimethamine and Dihydroartemesinin, are routinely tested on each Pf assay plate with two-fold purpose; to check the quality and reproducibility of the assay and to act as positive controls. None of the compounds tested showed a potency comparable to that of the standard molecules, but those with sub-micromolar potency

could be considered suitable for further investigation and development. Two erythrocyte densities were tested to determine if erythrocyte density affects potency. While we did observe some differences, in general they were minor and non-significant, indicating that there is no series-wide effect of erythrocyte density on compound potency.

Compound	<i>Plasmodium falciparum</i> (5% Haematocrit) *			<i>Plasmodium falciparum</i> (1.25% Haematocrit) *			HepG2 (toxicity)	n	$\beta$ -Hematin formation inhibition **
	EC <sub>50</sub> ( $\mu$ M)	EC <sub>50</sub> conf interval		EC <sub>50</sub> ( $\mu$ M)	EC <sub>50</sub> conf interval		EC <sub>50</sub> ( $\mu$ M)		
<b>1</b>	0.32	0.30	0.34	0.43	0.33	0.60	> 10	4	78.7 $\pm$ 0.057
<b>2</b>	0.22	0.17	0.29	0.51	0.47	0.57	> 10	4	66.3 $\pm$ 0.173
<b>3</b>	0.59	0.57	0.61	0.47	0.41	0.55	> 10	4	5.1 $\pm$ 0.088
<b>4</b>	0.33	0.30	0.37	0.17	0.13	0.25	> 10	4	79.4 $\pm$ 0.152
<b>5</b>	2.51	2.50	2.53	0.42	0.28	0.70	> 10	4	25.6 $\pm$ 0.120
<b>6</b>	0.27	0.27	0.28	0.78	0.42	1.84	> 10	4	11.3 $\pm$ 0.066
<b>7</b>	0.82	0.78	0.89	0.21	0.062	1.15	> 10	4	5.8 $\pm$ 0.080
<b>8</b>	2.36	2.31	2.43	0.62	0.49	0.85	> 10	4	7.5 $\pm$ 0.040
<b>9</b>	1.29	1.29	1.30	0.47	0.34	0.74	> 10	4	8.4 $\pm$ 0.014
Mefloquine	0.032	0.020	0.049	0.019	0.013	0.028			
Pyrimethamine	0.029	0.027	0.032	0.026	0.014	0.049			
Dihydroartemesinin	0.013	0.011	0.015	0.004	0.002	0.007			
Chloroquine									33.2 $\pm$ 0.145

\* Each assay was run in duplicate. \*\* Assay was run in triplicate.

**Table 1.** EC<sub>50</sub> ( $\mu$ M) with 95% confidence intervals, from testing of the isolated hydroxyquinoline (**1-7**) and hydroxyquinolone (**8-9**) in *P. falciparum*, and HepG2 toxicity assay.

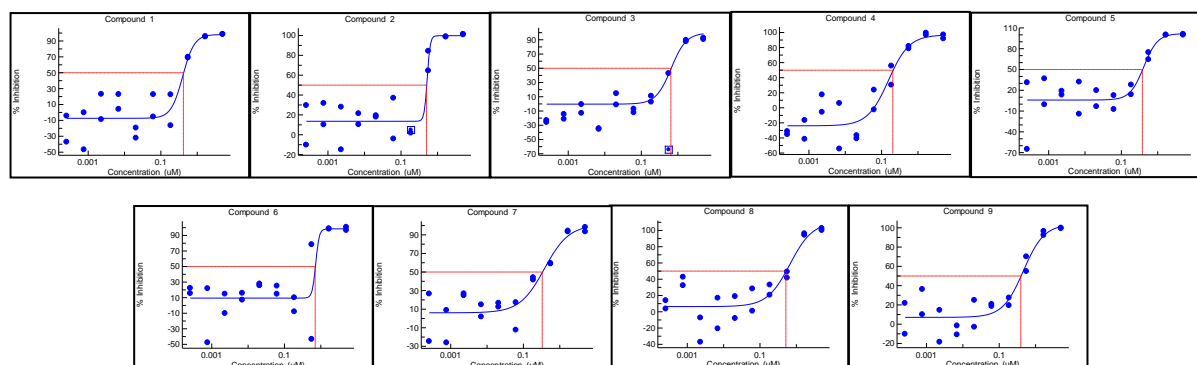
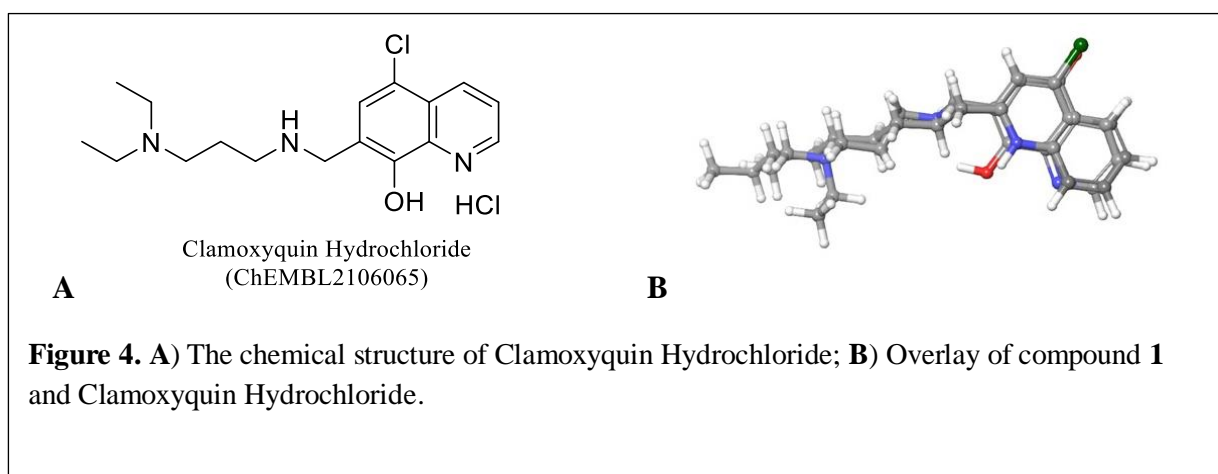


**Figure 3.** EC<sub>50</sub> ( $\mu$ M) potency curves for compounds **1-9** in 1.25% Haematocrit *P. falciparum* *in vitro* assay.

### 3.3. Identification of potential Pf drug targets by similarity search

In this approach, we used shape screening of compound **1** against the ChEMBL database. We identified clamoxyquin hydrochloride (ChEMBL2106065) as the most similar compound to compound **1** as shown in Figure 4. Clamoxyquin hydrochloride is an antiamebic and antidiarrheal drug used to treat salmonids for infection with the myxozoan parasite *Myxobolus cerebralis* [19]. Given the high structural similarity between clamoxyquin and the antimalarial drug chloroquine, we investigated the hypothesis that our compounds may act in a similar mechanism of action to chloroquine [20]. Chloroquine act by inhibiting the hemozoin ( $\beta$ -hematin) formation [21, 22] thereby resulting in the accumulation of heme which is toxic to the malaria parasite. To determine if the isolated compounds also target hemozoin resulting in heme accumulation, we investigated their effect on  $\beta$ -hematin formation.



### 3.4. *In vitro* evaluation of inhibition of $\beta$ -hematin formation

Hemozoin is an aggregate of hematin (oxidised heme) produced upon haemoglobin digestion by hematophagous organisms. It is the primary mechanism of heme detoxification in several blood-feeding organisms, including *Plasmodium* [23], *Schistosoma* [24], *Haemoproteus columbae* [25] and *Rhodnius prolixus* [26]. Free heme (ferriprotoporphyrin IX) is toxic to the parasites because it can peroxidate lipids, produce oxygen radicals, inhibit enzyme activities and damage cell membranes [27, 28]. Hence, how to dispose free heme is of central importance in the physiological processes of hematophagous

organisms. To detoxify the free heme, the malaria parasites convert it into insoluble crystals, known as hemozoin. Since hemozoin formation is essential for these parasites survival, inhibiting hemozoin aggregation represents an attractive drug target [26].

All the tested compounds inhibited  $\beta$ -hemozoin formation with  $IC_{50}$  values less than 100  $\mu$ M. Moreover, six out of the nine screened compounds showed inhibition with  $IC_{50}$  values less than that of chloroquine ( $33.2 \pm 0.145$ , Table 1;  $31.5 \pm 0.5$  [33]) and quinine ( $52 \pm 0.9$ ; [30]), antimalarial drugs already known to target hemozoin formation further confirming that the compounds target the process of hemozoin formation. Compounds **3**, and **6-9** exhibited significant inhibition of  $\beta$ -hemozoin formation with  $IC_{50}$  values 5.1, 11.3, 5.8, 7.5 and 8.5  $\mu$ M respectively which are 6-8 fold higher activity than chloroquine (Table 1). Surprisingly, not all compounds with the high  $\beta$ -hemozoin inhibitory activity did result in high antimalarial activity (Table 1) confirming the screened compounds could act on more than one target in the malaria parasite which requires future investigation.

### 3.5. Structure-Activity Relationships (SARs)

Quinolines are privileged scaffolds in medicinal chemistry and have a broad-spectrum of biological activities. For example, they showed anticancer, antiviral, antileishmanial, and antimalarial properties [31]. Quinoline is the core scaffold of the known antimalarial drugs, chloroquine and quinine (Figure 1). The core structure of the nine isolated natural products is the quinoline ring system.

Compounds **1-3** are 4-hydroxyquinolines substituted at position-2 with two unbranched saturated aliphatic chains [C7 (i.e. **1**) and C9 (i.e. **2**)] and C9 monounsaturated aliphatic chain (i.e. **3**). Compound **2** was the most active against *P. falciparum* (5% Haematocrit) ( $EC_{50} = 0.17 \mu$ M) but showed low activity toward  $\beta$ -hemozoin formation ( $IC_{50} = 66.30 \mu$ M). Compounds **2** and **3** showed good activity toward *P. falciparum* (5% and 1.25% Haematocrit) while compound **3** was the most active against  $\beta$ -hemozoin formation ( $IC_{50} = 6.10 \mu$ M).

The 4-hydroxyquinoline-*N*-oxide is the core scaffold of compounds **4-7**. These compounds are substituted at position-2 with saturated C7 (i.e. **4**), saturated C9 (i.e. **5**), monounsaturated C9 (i.e. **6**), monounsaturated C11 (i.e. **7**). Compound **6** substituted with the monounsaturated C9 was >9-fold more

active than compound **5** substituted with saturated C9 when tested against *P. falciparum* (5% Haematocrit). Moreover, **6** was >2-fold more active than **5** when tested against  $\beta$ -hematin formation, which suggested that the monounsaturated C9 is more favoured than the saturated analogue. On the other hand, compound **7** with monounsaturated C11 substituent showed high potency ( $EC_{50} = 0.062 \mu\text{M}$ ) when tested against *P. falciparum* (1.25% Haematocrit) and was the most active one in this series (i.e. **4-7**) toward  $\beta$ -hematin formation ( $IC_{50} = 5.80 \mu\text{M}$ ), and was comparable to compound **3** in its activity toward this target.

Both hydroxyquinoline-2,4-dione (**8**) and hydroxyquinolinone (**9**) showed lower activity toward *P. falciparum* (5% Haematocrit), and good activity toward *P. falciparum* (1.25% Haematocrit). Additionally, both compounds showed good activity toward  $\beta$ -hematin formation ( $IC_{50} = 7.50$  and  $8.40 \mu\text{M}$  for **8** and **9**, respectively).

## Conclusion

In conclusion, we have isolated seven hydroxyquinoline and two hydroxyquinolone derivatives from the rhizobacterium *P. agglomerans* and tested their activity against one of the major malarial causative agents, *P. falciparum*. Selective activity at sub-micromolar level against Pf under high throughput screening led to computational investigation for drug target validation where hemozoin was identified as one possible target for our compounds in Pf. The computationally validated target was further rectified by *in vitro* analysis, and the competitive inhibitory effect of six out of the nine identified compounds showed greater activity than the control drug chloroquine. Based on our data, compounds **8** and **9** are the most promising hits for future optimisation. We will establish primary structure-activity relationships of identified compounds through analog design to enhance potency and achieve satisfactory ADME and optimal physicochemical properties. Following establishment of SAR, we will develop quantitative structure-activity relationships (QSAR) model to guide our design process.

**Supplementary data:** Supplementary data to this article can be found online at XXX.

**Declaration of Competing Interest:** The authors declare that they have no known competing financial interests or personal relationships that could have appeared to influence the work reported in this paper.

**Funding:** This research did not receive any specific grant from funding agencies in the public, commercial, or not-for-profit sectors.

## References

- [1]. Elliott, E., Chassagne, F., Aubouy, A., Deharo, E., Souvanasy, O., Sythamala, P., Sydara, K., Lamxay, V., Manithip, C., Torres, J.A. and Bourdy, G., 2020. Forest Fevers: traditional treatment of malaria in the southern lowlands of Laos. *Journal of Ethnopharmacology*, 249, 112187, doi.10.1016/j.jep.2019.112187.
- [2]. Noedl, H., Se, Y., Schaefer, K., Smith, B.L., Socheat, D. and Fukuda, M.M., 2008. Evidence of artemisinin-resistant malaria in western Cambodia. *New England Journal of Medicine*, 359 (24), pp.2619-2620.
- [3]. Dondorp, A.M., Nosten, F., Yi, P., Das, D., Physo, A.P., Tarning, J., Lwin, K.M., Ariey, F., Hanpithakpong, W., Lee, S.J. and Ringwald, P., 2009. Artemisinin resistance in *Plasmodium falciparum* malaria. *New England Journal of Medicine*, 361(5), pp.455-467.
- [4]. Ocan, M., Akena, D., Nsoyba, S., Kanya, M.R., Senono, R., Kinengyere, A.A. and Obuku, E., 2019. K13-propeller gene polymorphisms in *Plasmodium falciparum* parasite population in malaria affected countries: a systematic review of prevalence and risk factors. *Malaria journal*, 18(1), 60, doi.10.1186/s12936-019-2701-6.
- [5]. Boni, M. F., Smith, D. L., and Laxminarayan, R., 2008. Benefits of using multiple first-line therapies against malaria. *Proceedings of the National Academy of Sciences*, 105, pp.14216-14221.
- [6]. Fairhurst, R. M., and Dondorp, A. M., 2016. Artemisinin-resistant *Plasmodium falciparum* malaria. *Microbiology spectrum*. 4(3), doi.10.1128/microbiolspec.EI10-0013-2016.
- [7]. Newman, D.J. and Cragg, G.M., 2020. Natural products as sources of new drugs over the nearly four decades from 01/1981 to 09/2019. *Journal of Natural Products*, 83(3), pp.770-803.
- [8]. Newman, D.J. and Cragg, G.M., 2016. Natural products as sources of new drugs from 1981 to 2014. *Journal of natural products*, 79, pp.629-661.
- [9]. Pidot, S.J., Coyne, S., Kloss, F. and Hertweck, C., 2014. Antibiotics from neglected bacterial sources. *International Journal of Medical Microbiology*, 304, pp.14-22.
- [10]. Cherif-Silini, H., Thissera, B., Bouket, A.C., Saadaoui, N., Silini, A., Eshelli, M., Alenezi, F.N., Vallat, A., Luptakova, L., Yahiaoui, B., Cherrad, C., Vacher, V., Al-Anzi, B.S., Rateb, M.E., Belbahri, L. 2019. Durum Wheat Stress Tolerance Induced by Endophyte *Pantoea agglomerans* with Genes Contributing to Plant Functions and Secondary Metabolite Arsenal. *Int. J. Mol. Sci.* 20, 3989; doi: 10.3390/ijms20163989.

- [11]. Smits, T.H., Rezzonico, F., Kamber, T., Goesmann, A., Ishimaru, C.A., Stockwell, V.O., Frey, J.E. and Duffy, B., 2010. Genome sequence of the biocontrol agent *Pantoea agglomerans* strain C9-1. *Journal of bacteriology*, 192(24), pp.6486-6487.
- [12]. Shibeshi, M.A., Kifle, Z.D. and Atnafie, S.A., 2020. Antimalarial drug resistance and novel targets for antimalarial drug discovery. *Infection and Drug Resistance*, 13, pp. 4047–4060.
- [13]. Supong, K., Thawai, C., Supothina, S., Auncharoen, P., and Pittayakhajonwut, P., 2016. Antimicrobial and anti-oxidant activities of quinoline alkaloids from *Pseudomonas aeruginosa* BCC76810. *Phytochemistry Letters*, 17, pp.100-106.
- [14]. Thissera, B., Alhadrami, H.A., Hassan, M.H., Hassan, H.M., Bawazeer, M., Yaseen, M., Belbahri, L., Rateb, M.E. and Behery, F.A., 2020. Induction of cryptic antifungal pulicatin derivatives from *Pantoea agglomerans* by microbial co-culture. *Biomolecules*, 10(2), 268, doi.10.3390/biom10020268.
- [15]. Baragaña, B., Hallyburton, I., Lee, M.C., Norcross, N.R., Grimaldi, R., Otto, T.D., Proto, W.R., Blagborough, A.M., Meister, S., Wirjanata, G. and Ruecker, A., 2015. A novel multiple-stage antimalarial agent that inhibits protein synthesis. *Nature*, 522(7556), pp.315-320.
- [16]. Bennett, T.N., Paguio, M., Gligorijevic, B., Seudieu, C., Kosar, A.D., Davidson, E. and Roepe, P.D., 2004. Novel, rapid, and inexpensive cell-based quantification of antimalarial drug efficacy. *Antimicrobial agents and chemotherapy*, 48(5), pp.1807-1810.
- [17]. Kitamura., S., Hashizume., K, Iida., K, Miyashita., E, Shirahata., K, Kase., H., 1986..II. KF8940 (2-n-Heptyl-4-hydroxyquinoline-N-oxide), a potent and selective inhibitor of 5-lipoxygenase, produced by *Pseudomonas methanica*. *The Journal of Antibiotics*. 39, pp.1160-1166.
- [18]. Hodgkinson, J. T., Galloway, W. R. J. D., Saraf, S., Baxendale, I. R., Ley, S. V., Ladlow, M., Welch, M., and Spring, D. R., 2011. Microwave and flow syntheses of *Pseudomonas* quinolone signal (PQS) and analogues. *Organic & Biomolecular Chemistry*. 9, pp.57-61.
- [19]. Sharma, A; Anand, N. 1997. Chapter 17-Quinolines. *Pharmacochemistry Library*.25, pp.393-420.
- [20]. Guerra, E.D., Baakdah, F., Georges, E., Bohle, D.S. and Cerruti, M., 2019. What is pure hemozoin? A close look at the surface of the malaria pigment. *Journal of inorganic biochemistry*, 194, pp.214-222.
- [21]. Fong, K.Y. and Wright, D.W., 2013. Hemozoin and antimalarial drug discovery. *Future medicinal chemistry*, 5(12), pp.1437-1450.
- [22]. Herraiz, T., Guillén, H., González-Peña, D. and Arán, V.J., 2019. Antimalarial Quinoline Drugs inhibit  $\beta$ -Hematin and increase free Hemin catalysing peroxidative Reactions and inhibition of cysteine proteases. *Scientific reports*, 9 (15398) doi.10.1038/s41598-019-51604-z.
- [23]. Noland, G.S., Briones, N. and Sullivan Jr, D.J., 2003. The shape and size of hemozoin crystals distinguishes diverse *Plasmodium* species. *Molecular and biochemical parasitology*, 130(2), pp.91-99.
- [24]. Oliveira, M.F., Kycia, S.W., Gomez, A., Kosar, A.J., Bohle, D.S., Hempelmann, E., Menezes, D.,

Vannier-Santos, M.A., Oliveira, P.L. and Ferreira, S.T., 2005. Structural and morphological characterisation of hemozoin produced by *Schistosoma mansoni* and *Rhodnius prolixus*. *Febs letters*, 579(27), pp.6010-6016.

[25]. Chen, M.M., Shi, L. and Sullivan Jr, D.J., 2001. *Haemoproteus* and *Schistosoma* synthesise heme polymers similar to *Plasmodium* hemozoin and  $\beta$ -hematin. *Molecular and biochemical parasitology*, 113(1), pp.1-8, doi.10.1016/S0166-6851(00)00365-0.

[26]. Stiebler, R., Hoang, A.N., Egan, T.J., Wright, D.W. and Oliveira, M.F., 2010. Increase on the initial soluble heme levels in acidic conditions is an important mechanism for spontaneous heme crystallisation in vitro. *PLoS One*, 5(9), p.e12694.

[27]. Aft RL, Mueller GC. 1984. Hemin-mediated oxidative degradation of proteins. *Journal of Biological Chemistry*. 259, pp.301–305.

[28]. Aft, R.L. and Mueller, G.C., 1983. Hemin-mediated DNA strand scission. *Journal of Biological Chemistry*, 258(19), pp.12069-12072.

[29]. Wicht, KJ, Combrinck, JM, Smith, PJ, Hunter, R, Timothy JE. 2016. Identification and SAR Evaluation of Hemozoin-Inhibiting Benzamides Active against *Plasmodium falciparum*. *Journal of Medicinal Chemistry*. 59 (13), pp.6512-6530.

[30]. Woodland. J, Hunter,R, Smith, PJ; Egan, TJ. 2017. Shining new light on ancient drugs: preparation and subcellular localisation of novel fluorescent analogues of *Cinchona* alkaloids in intraerythrocytic *Plasmodium falciparum*. *Organic and Biomolecular Chemistry*. 15, pp.589–597.

[31]. Jakubczyk, D., Pfau, R., Encinas, A., Rösch, E., Gil, C., Masters, K., Gläser, F., Kramer, C.S., Newman, D., Albericio, F. and Steinhagen, H., 2015. *Privileged scaffolds in medicinal chemistry: design, synthesis, evaluation*. Royal Society of Chemistry. doi.10.1039/9781782622246.